Molecular Vision 2007; 13:1701-10 <http://www.molvis.org/molvis/v13/a190/>
Received 23 May 2007 | Accepted 15 September 2007 | Published 18 September 2007

Electroretinographic analyses of Rpe65-mutant *rd12* mice: Developing an in vivo bioassay for human gene therapy trials of Leber congenital amaurosis

Alejandro J. Roman,[1] Sanford L. Boye,[2] Tomas S. Aleman,[1] Ji-jing Pang,[2] J. Hugh McDowell,[2] Shannon E. Boye,[2] Artur V. Cideciyan,[1] Samuel G. Jacobson[1], William W. Hauswirth[2]

[1]Department of Ophthalmology, Scheie Eye Institute, Philadelphia, PA, [2]Department of Ophthalmology, University of Florida, Gainesville, FL

Purpose: Dramatic restoration of retinal function has followed subretinal viral-mediated gene therapy in RPE65-deficient animal models of human Leber congenital amaurosis (LCA) caused by *RPE65* mutations. Progress in early-phase clinical trials of *RPE65*-LCA prompted us to begin development of an in vivo bioassay of clinical grade vector stability for later-phase trials.

Methods: Naturally-occurring Rpe65-mutant *rd12* mice (2-4 mo of age) were studied with full-field electroretinograms (ERGs). Flash stimuli (range, -4.1 to 3.6 log scot-cd.s.m^{-2}) were used to evoke ERGs in anesthetized, dark-adapted mice. B-wave amplitudes were measured conventionally and luminance-response functions were fit. Leading edges of photoresponses were analyzed with a model of rod phototransduction activation. A unilateral subretinal injection of AAV2-CB^{SB}-h*RPE65* vector was delivered and therapeutic efficacy of 4 doses spanning a 2 log unit range was studied with ERGs performed about 6 weeks after injection. Uninjected *rd12* eyes and wild-type (wt) mice served as controls.

Results: *Rd12* mice showed substantially smaller amplitudes and lower sensitivities than wt mice for all measured ERG b-wave and photoresponse parameters. For the dose-response study, there was no difference between 0.01X-dosed mice and untreated mutants. Improved receptoral and post-receptoral function was evident for 0.1X, 0.3X, 1X doses: b-wave semi-saturation constants decreased, b-wave amplitudes increased with dose; photoresponses showed faster kinetics and higher maximum amplitudes. ERG b-wave amplitude to a selected stimulus light intensity could provide evidence of biologic activity of the vector; interocular differences in b-wave amplitude comparing treated versus untreated eyes in the same animal also revealed vector efficacy.

Conclusions: We have taken the first steps toward developing an ERG assay of biologic activity of human grade vector for future clinical trials of *RPE65*-LCA. Faithful murine models of treatable human disease tested with specific ERG protocols may emerge as valuable in vivo bioassays for future human clinical trials of therapy in many retinal degenerative diseases.

RPE65 (retinal pigment epithelium-specific 65 kDa protein) is the isomerohydrolase of the visual (retinoid) cycle [1-3], the pathway that regenerates visual pigment after light is absorbed [4]. Mutations in the *RPE65* gene are known to cause Leber congenital amaurosis (LCA), a severe early-onset blinding human disease [5,6]. Longstanding scientific interest in details of the visual cycle, the availability of naturally-occurring and genetically-engineered animals with RPE65 deficiency, and relevance to human blindness has accelerated scientific and medical activity toward initiating gene therapy clinical trials in *RPE65*-LCA. Systematic steps have been taken toward human trials. Proof-of-concept studies with viral gene transfer of *RPE65* have occurred in dogs [7-11], and in mice [12-17]. Dose-response and safety studies have been performed in dogs and non-human primates [18,19]. Human studies have inquired whether the successfully-treated animals with RPE65 deficiency sufficiently model the human disease to warrant translation to the clinic [20], and what outcome measures would accommodate the severe visual loss and nystagmus in the *RPE65*-LCA patients [21-23].

The steady progress toward early-phase human clinical trials of *RPE65*-LCA prompted us to begin considering the needs of later-phase trials. One such need will be an analytical method to determine whether the clinical grade gene therapy agent is biologically active [24,25]. Building upon the foundation of studies to date, we chose to explore an in vivo assay of biologic activity using a surrogate measure of gene expression in an available murine model with Rpe65 deficiency. The measurement tool is the electroretinogram (ERG), the time-honored non-invasive retinal function test used in the clinic [26,27], in the laboratory to determine retinal phenotype in mice [28-30], and in proof-of-concept studies of vector-mediated gene therapy in Rpe65-deficient mice [12-17].

First, we defined the ERG abnormality of the naturally-occurring *rd12* mouse model of Rpe65 deficiency [12-17,31-38]. Then, we quantified ERG parameters at different doses

Correspondence to: Samuel G Jacobson, MD 51 N 39th Street, Philadelphia, PA 19104. Phone: (215) 662-9981; FAX: (215) 662-9388; email: jacobsos@mail.med.upenn.edu

of AAV2 vector containing human *RPE65* cDNA delivered by subretinal injection [18,19]. The results lead to suggestions for bioassays of clinical grade vector for future late-phase clinical trials of *RPE65*-LCA.

METHODS

Animals: Rd12 (N=39; 16 female and 23 male) and normal wildtype (wt, N=10; 1 female; 9 male) C57BL/6J mice were used in this study. Mice were generated from breeding pairs obtained from the Jackson Laboratories (Bar Harbor, ME) and were 2 to 4 mo of age at the time of testing. Animals were kept in cages (average 2-3 animals per cage) under 12 h-on/12-h-off cyclic lighting (ambient illumination 75 lx), with lights on at 7 am. Access to food (LM-485, Harlan Teklad, Madison, WI) and water was ad libitum. Procedures were conducted in accordance with the ARVO Statement for the Use of Animals in Ophthalmic and Visual Research and with institutional approval.

Electroretinography: Full field bilateral ERGs were recorded using a custom-built ganzfeld, a computer-based system (EPIC-XL, LKC Technologies, Gaithersburg, MD) and specially-made contact lens electrodes (Hansen Ophthalmics, Iowa City, IA). Animals were dark-adapted (>12 h) and anesthetized with a mixture of ketamine HCl (65 mg/kg) and xylazine (5 mg/kg) intramuscularly under dim red light. Corneas were anesthesized with proparacaine HCl, and pupils were dilated with tropicamide (1%) and phenylephrine (2.5%). Medium energy (10 μs duration) and high energy (1 ms duration) flash stimulators with unattenuated luminances of 0.8 and 3.6 log scot-cd.s.m^{-2}, respectively, were used. Neutral density (Wratten 96) and blue (Wratten 47A) filters served to attenuate and spectrally-shape the stimuli. The signals evoked by medium energy flashes were amplified, filtered (-3 dB cutoff at 0.3 and 300 Hz) and digitized (2 kHz) with an 12-bit analog-to-digital converter. Signals evoked by higher energy flashes were recorded with higher bandwidth (1500 Hz filtering and 3.33 kHz sampling).

First, dark-adapted ERGs were obtained with increasing intensities of blue light flashes from -4.2 to 0.1 log scot-cd.s.m^{-2}. Dimmer intensities were presented at 0.5 Hz and 10 waveforms were averaged; brighter intensities were presented at 0.1 Hz and 2 waveforms were averaged. Intensity increments were in 0.3-0.5 log unit steps. Next, an ERG photoresponse was evoked with a single blue 2.2 log scot-cd.s.m^{-2} flash. A 2-min wait served to permit complete recovery of the photoresponse. Then a single white 3.6 log scot-cd.s.m^{-2} flash was used to evoke the maximal photoresponse.

B-wave amplitudes were measured conventionally, from baseline or a-wave trough to positive peak, and fit with a Naka-Rushton function [39,40] to obtain estimates of maximum amplitude (V_{max}) and sensitivity (semisaturation intensity, log K). A derived parameter, log(V_{max}/K), was used to succinctly represent overall post-receptoral function. Leading edges (4 to 20 ms, depending on the response) of the two photoresponses were fitted as an ensemble with a model of rod phototransduction activation [12,32,39,41] and maximum amplitude (R_{max}) and sensitivity (log S) parameters were derived. A derived parameter, log(R_{max}*S), was used to represent overall photoreceptor function.

Efficacy of the treatment was statistically evaluated considering the derived ERG parameters, log(R_{max}*S) and log(V_{max}/K), in injected and control eyes. A one-way analysis of variance (ANOVA) with repeated measures was employed to adjust for the possible correlation between the eyes of each animal. When the overall difference among 5 groups of eyes was statistically significant, post-hoc pair-wise comparisons were performed between injected eyes at each dose level with control eyes. Additionally, test of linear trend was performed for each variable. Computations were executed on the statistical software SAS (version 9.1, SAS Institute, Inc., Cary, NC).

Efficacy of the treatment was alternatively evaluated by estimating the fraction of injected eyes (at each dose) that show an ERG parameter substantially better than what would be expected from uninjected eyes. The four ERG parameters (R_{max}, log S, V_{max}, and log K) were individually evaluated using a conservative criterion of mean±3SD derived from control eyes [9]. Additionally, a parameter consisting of the interocular difference (IOD) of b-wave amplitude evoked by a 0.1 log scot-cd.s.m^{-2} blue flash was considered as a simpler and shorter methodology for a potential bioassay. For this analysis, IOD limits (mean+3SD) were first defined for smaller amplitude *rd12* records (21 μV IOD at a mean amplitude of 16 μV) and larger amplitude wt records (284 μV IOD at a mean amplitude of 356 μV) in animals with bilateral ERG recordings and no treatment. Treatment efficacy in the injected *rd12* eyes was determined using a criterion that was dependent on the amplitude of the uninjected eye and was derived from the linear interpolation of IOD limits between the *rd12* and wt results.

Vector and injection: A single 1 μl subretinal injection of a serotype 2 AAV vector containing the human *RPE65* cDNA (rAAV2-CB^{SB}-h*RPE65*) was delivered to one eye (N=34) of *rd12* mice at an average age of 3.3 weeks (range, 2 to 5.3). The construct and dosage of vector was based on previous studies [18,19]. Four vector doses were studied over a two log unit range: 0.01X (N=5), 0.1X (N=10), 0.3X (N=11) and 1X (N=8) where 1X corresponded to 10^{10} vg/ μl. The remaining five *rd12* mice were not treated. All uninjected *rd12* eyes (N=44) served as controls.

RESULTS

Rpe65-deficient rd12 *mouse electroretinography parameters:* Waveforms recorded to increasing intensities of light stimuli from two-month-old normal wt (left) and *rd12* (right) mice are illustrated (Figure 1A). ERG b-waves of the *rd12* mouse were not detectable below an intensity of -0.8 log scot-cd.s.m^{-2}, but intensities at and above 0.1 log scot-cd.s.m^{-2} can evoke recordable and sometimes sizeable responses. Of note, there were small and slow but detectable a-waves in mutant eyes at higher intensities [32]. Leading edges of these a-waves evoked by 2.2 and 3.6 log scot-cd.s.m^{-2} intensities directly assess photoreceptor activation kinetics and were fit with a model of phototransduction activation (Figure 1B). Compared to wt, *rd12* mice showed a-waves (also called ERG photoresponses) with a significant reduction of maximum amplitude and slower

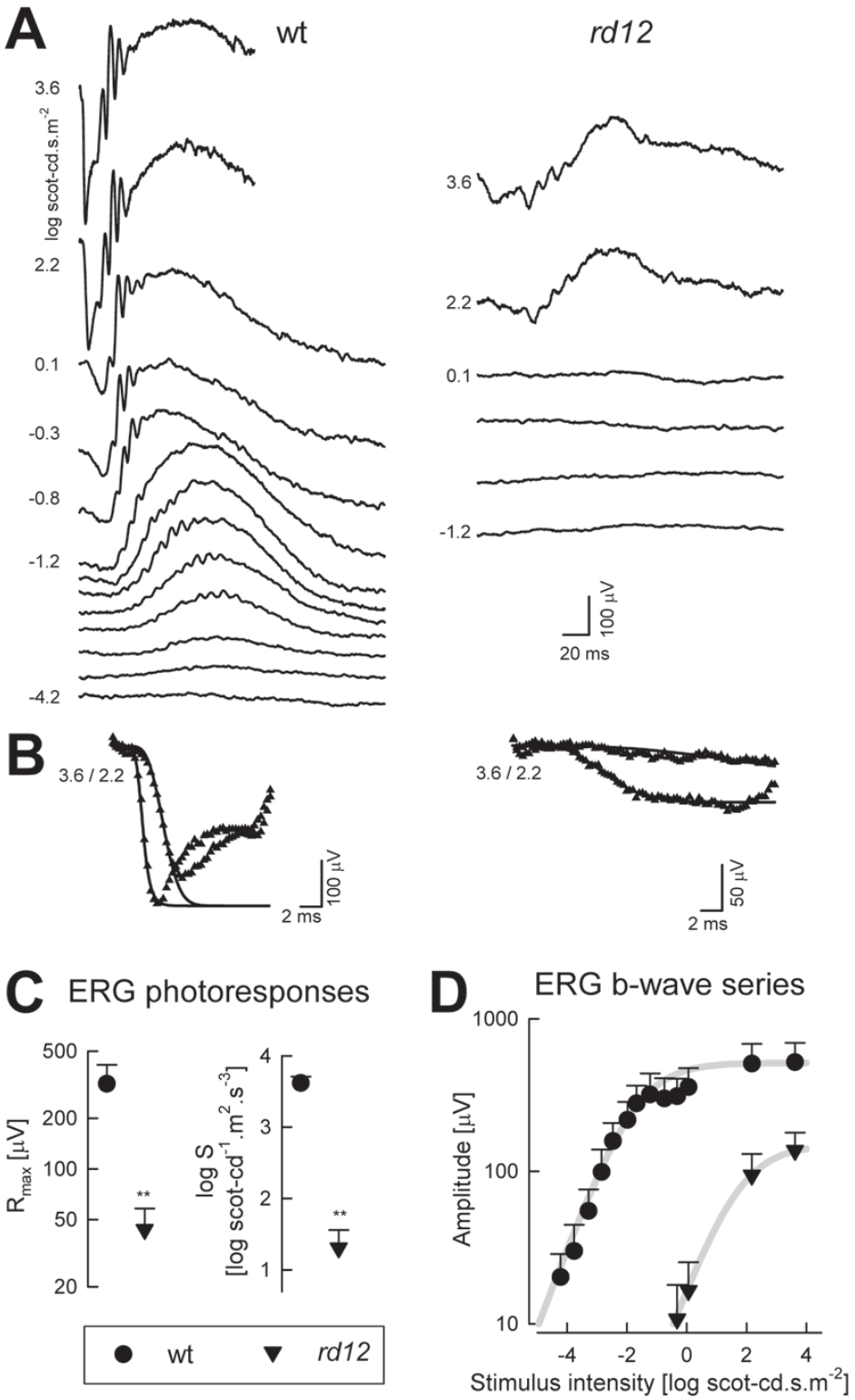

Figure 1. Definition of electroretinography abnormalities in the *rd12* mouse model of *RPE65*-LCA. **A**: Dark adapted ERGs to increasing stimulus intensities (shown to the left of key traces) for representative 2-month-old wt and *rd12* mice. Blue flashes were used for all intensities except the highest, which were evoked by white flashes. Traces start at stimulus onset. **B**: ERG photoresponses (symbols) evoked by 3.6 and 2.2 log scot-cd.s.m^{-2} flashes are fit as an ensemble with a model of phototransduction (smooth lines). The response from the mutant shows reduced amplitude and sensitivity. **C**: Summary statistics of maximum amplitude (R_{max}) and sensitivity (log S) parameters obtained from photoresponse modeling in *rd12* mice are significantly (*) different than wt. **D**: Luminance-response functions derived from ERG b-wave series show diminished light sensitivity in mutant animals indicated by a shift to the right of the curves. Mutant animals also show a reduction in maximum amplitude. Error bars equals to 1SD.

response kinetics. The prominent retinal function abnormalities were consistent with previous reports in *rd12* [14,17,37,38] and *Rpe65-/-* mice [12,13,31-36].

A summary of the phototransduction activation parameters, maximum amplitude (R_{max}) and sensitivity (log S), obtained by modeling of the leading edges of the ERG photoresponses is shown (Figure 1C). Mean (±SD) R_{max} was 320 (±94) µV for wt and 40 (±15) µV for *rd12*; log S values were 3.62 (±0.36) and 1.32 (±0.27) log scot-cd^{-1}.m^2.s^{-3} for wt and *rd12*, respectively (p<0.001 for both). Overall photoreceptor function as estimated by log(R_{max}*S) was significantly depressed by 3.2 log units in *rd12* mice compared to wt.

Dark-adapted ERG b-waves originate primarily from the activity of bipolar cells driven by photoreceptor cells [42,43]. Luminance-response functions obtained from ERG b-wave series can thus parameterize the post-receptoral function to a good first approximation [39]. Even though b-wave amplitudes in some *rd12* mice could be sizeable at the higher intensity stimuli (Figure 1A), there were significant differences between *rd12* and wt mice (Figure 1D). Average b-wave luminance-response function fit with a Naka-Rushton equation (Figure 1D, gray lines) was significantly right-shifted in *rd12* compared to wt mice. Log K values were -1.45±0.43 and 1.86±0.38 log scot-cd.s.m^{-2}, for wt and *rd12*, respectively, corresponding to a 3.3 log unit loss of light sensitivity due to the Rpe65 deficiency (Figure 1D). V_{max} was 518±176 µV in wt and 137±42 µV in *rd12*. *Rd12* mice showed pronounced impairment of overall post-receptoral function as estimated by log(V_{max}/K) showing a 3.8 log unit difference from wt.

Dose-response functions in rd12 *mice with subretinal injections of human grade AAV2-RPE65 vector:* Representative *rd12* mice evaluated 6.5 (range, 5.3 to 7.6) weeks after treat-

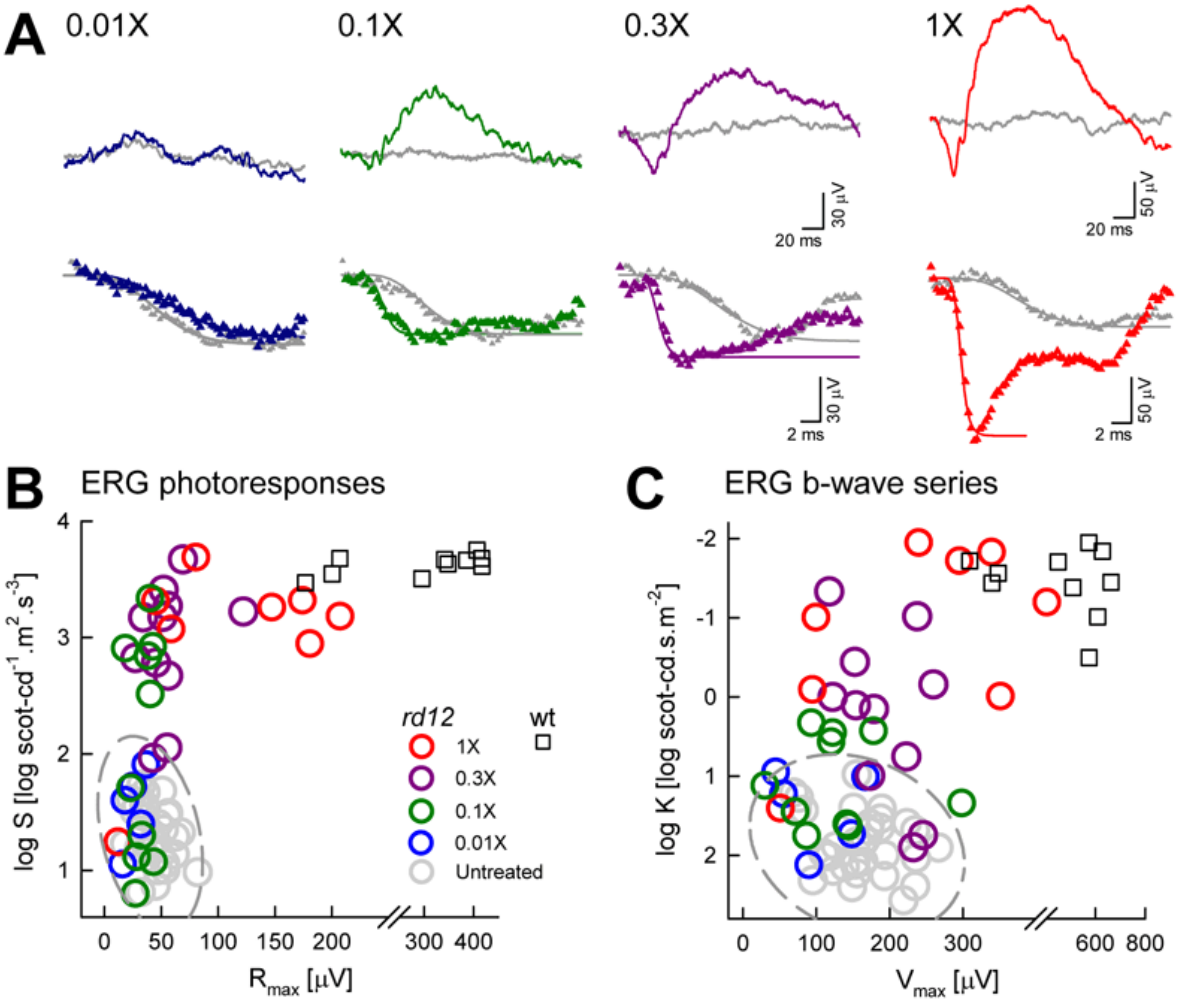

Figure 2. Electroretinography parameters of *rd12* mice to different doses of subretinal AAV2-hRPE65. **A**: ERGs evoked by 0.1 log scot-cd.s.m^{-2} flashes (upper row) and by 3.6 log scot-cd.m.s^{-2} flashes (lower row) in treated (colors) and untreated (gray) eyes of one *rd12* mouse from each dose group. As vector dose increases, responses become asymmetric with treated retinas showing increasing amplitude of b-waves and faster photoresponses. Photoreceptor activation models (smooth lines) fit to the photoresponses are shown. All traces start at stimulus onset. **B**: Photoresponse parameters in *rd12* eyes treated with a range of vector doses. As dosage increases above 0.01X, parameter pairs drift outside of the 99% confidence region (dashed ellipse) defined by the untreated eyes of *rd12* animals and start approaching wt levels. **C**: Luminance response parameters in treated *rd12* eyes similarly show a dose-related progression from the region corresponding to untreated eyes to the region corresponding to wt eyes.

ment demonstrate the effect of vector dose on ERG responses in the AAV2-h*RPE65* injected eyes (Figure 2A, colored traces) as compared to contralateral control eyes (Figure 2A, gray traces). At the lowest vector dose (0.01X) used in these studies, b-wave and photoresponse waveforms from the two eyes were indistinguishable and were not different from untreated *rd12* eyes. At higher doses, however, there were notable asymmetries between the eyes. Treated eyes had responses with greater b-wave amplitude and faster photoresponses with larger amplitudes.

Statistical analysis (one-way ANOVA with repeated measures) of the overall photoreceptor and post-receptoral ERG function showed highly significant differences among the groups of injected and control eyes ($p<0.0001$ for $\log(R_{max}*S)$ and $p=0.0003$ for $\log(V_{max}/K)$). Pairwise post-hoc comparison between the eyes at each dose level and control eyes showed significant improvement in both parameters at 0.1X, 0.3X and 1X (Table 1). Furthermore, there was a statistically significant dose response relationship for both parameters (P for linear trend, 0.0002 and 0.0003 for $\log(R_{max}*S)$ and $\log(V_{max}/K)$, respectively).

To understand better the physiologic basis of the treatment effect, photoreceptor activation parameters were compared between treated and untreated *rd12* eyes (Figure 2B). Photoreceptor activation of eyes treated with 0.01X dose (blue symbols) fell within the 99% confidence interval of untreated eyes (gray symbols). With increasing treatment dose between 0.1X and 1X, there was a gradual increase in photoresponse sensitivity (log S) such that some of the 0.3X and 1X eyes approached values from wt eyes. Additionally, many eyes receiving the highest doses showed a large increase in maximum amplitude (Figure 2B).

Post-receptoral function parameters derived from ERG b-wave series in treated *rd12* eyes also showed an orderly relationship with treatment dose (Figure 2C). At 0.01X dose, both sensitivity (log K) and maximum amplitude (V_{max}) parameters clustered within the 99% confidence interval of values obtained from untreated eyes. With increasing treatment dose, there was a gradual increase in log K. A fraction of *rd12* eyes treated with the 1X dose showed log K and V_{max} values approaching those of wt eyes.

Estimating treatment efficacy with electroretinography parameters: ERG data from individual treated eyes (Figure 2B,C) suggested that increasing dose was associated with increasing fraction of eyes showing a detectable treatment effect. To quantify this impression, the proportion of vector-injected eyes with ERG treatment efficacy are shown for each of the 4 doses tested (Figure 3A,B). A conservative criterion for efficacy was established from the limits (mean±3SD) of data from untreated eyes. Both photoresponse and b-wave sensitivity measures (log S and log K) demonstrated similar treatment efficacies, rising from 0% at 0.01X to 88% at 1X dose (Figure 3A,B). Maximum amplitude measures (R_{max} and V_{max}) on the other hand, showed little or no treatment efficacy at 0.01X, 0.1X and 0.3X doses but did rise to 40%-50% at 1X dose.

The dose-related increases in ERG sensitivity parameters suggested the possibility of using ERGs evoked by a flash carefully chosen to be near b-wave threshold in untreated *rd12* eyes. Based on the luminance-response function (Figure 1D), a stimulus intensity of 0.1 log scot-cd.s.m^{-2} was chosen. A left-shift of the luminance-response function due to efficacious treatment would be expected to increase the amplitude of this response potentially simplifying and shortening the experimental protocol. ERG b-wave amplitudes of treated eyes were plotted against untreated eyes and treatment efficacy was defined by expected interocular differences (IOD) of this amplitude in untreated *rd12* and wt eyes (Figure 3C). The resulting treatment efficacy curve (Figure 3D) was similar to that obtained from the log S parameter whether using IOD analysis (Figure 3D) or considering all untreated eyes as a control group (Figure 3A). IOD analysis of the other sensitivity parameter, log K, showed identical results (data not shown).

DISCUSSION

Naturally-occurring *rd12* mice with Rpe65 deficiency showed ERG b-wave features of severely reduced responsiveness to light, in concurrence with earlier studies [14,17,37,38]. Novel

Table 1. Comparison of ERG measures among different dose levels

		Dose					
ERG measure	Control (N=44)	0.01X (N=5)	0.1X (N=10)	0.3X (N=11)	1X (N=8)	Overall p-value	Linear trend p-value
Photoreceptor	2.89 (0.04)	2.92 (0.18)	3.56* (0.29)	4.64** (0.17)	4.93** (0.36)	<0.0001	0.0002
Postreceptor	0.34 (0.06)	0.49 (0.21)	0.98** (0.19)	2.02** (0.28)	3.08** (0.47)	0.0003	0.0003

The table includes mean (std.error) values for photoreceptor- and postreceptor-based ERG measures in each of the five groups of eyes as well as showing the statistical significance of the overall differences and linear trend. Photoreceptor measure corresponds to $\log(R_{max}*S)$ parameter derived from ERG photoresponses and it is specified in units of log μV. scot-cd^{-1}.m^{2}.s^{-3}. Postreceptor measure corresponds to $\log(V_{max}/K)$ parameter derived from ERG luminance response functions and it is specified in units of log μV. scot-cd^{-1}.m^{2}.s^{-1}. One-way ANOVA with repeated measures was used to evaluate overall differences which were highly significant. Both ERG parameters show a significant linear trend with dose suggesting a dose response relationship. Pairwise post-hoc comparisons are made between the eyes at each dose level and control eyes, and significance of the differences specified with asterisk: single asterisk corresponds to $0.01<p<0.05$, and double asterisk corresponds to $p<0.01$.

to the current study was the analysis of ERG photoresponses which are dominated by the phototransduction activation in photoreceptors [44,45]. *Rd12* mice showed substantially reduced photoresponse maximum amplitude and sensitivity parameters; the severity of dysfunction in *rd12* mice appeared to be slightly greater than that reported in *Rpe65-/-* mice [12,20,32]. Assuming isorhodopsin is responsible for remnant rod retinal function in these models [35,46], reduced

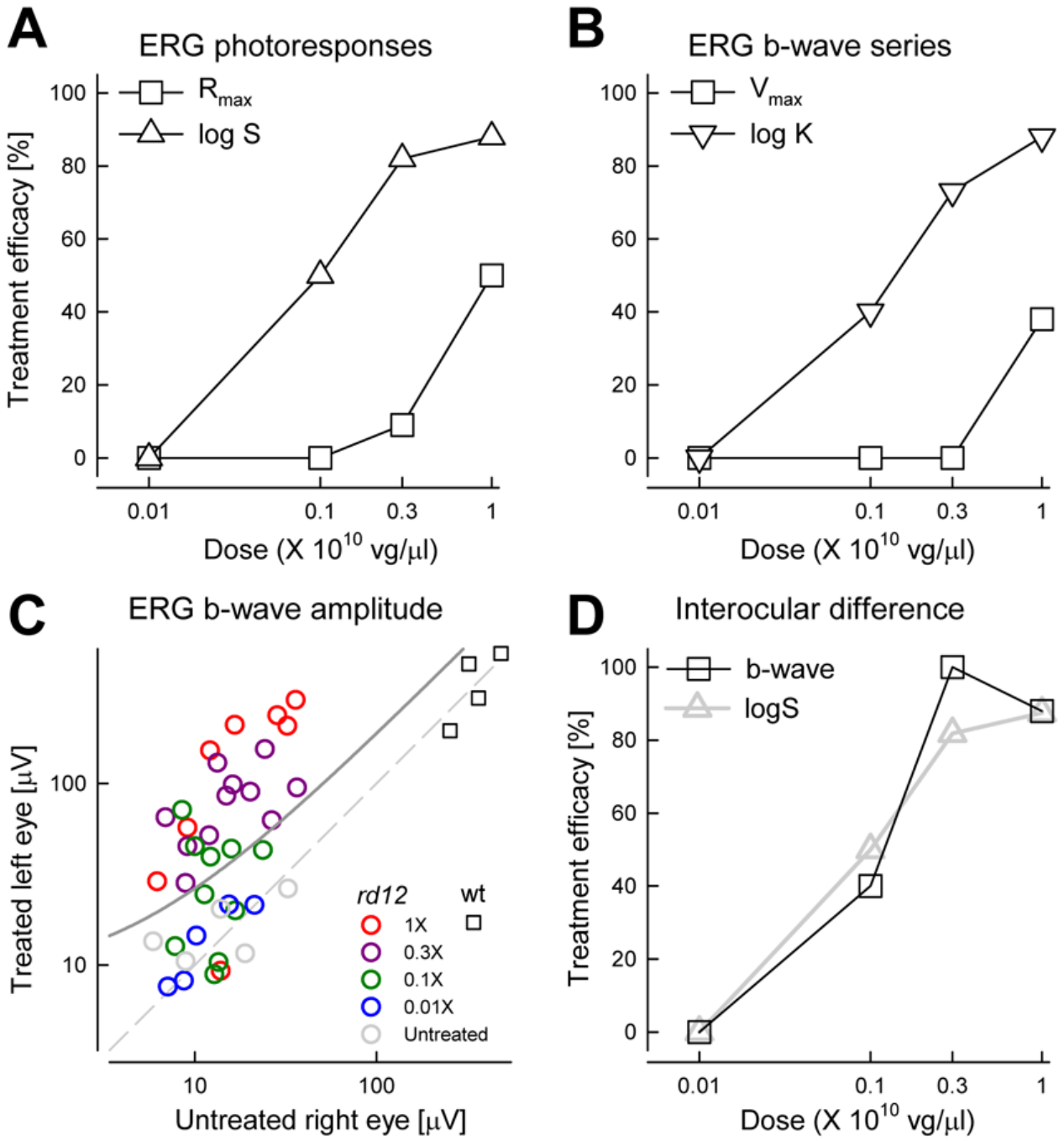

Figure 3. Treatment efficacy as a function of vector dose. **A**: Sensitivity (log S) parameter of ERG photoresponses detects efficacy at lower doses than the maximum amplitude (R_{max}) parameter. **B**: Sensitivity (log K) parameter of b-wave luminance-response function detects efficacy at lower doses than the maximum amplitude (V_{max}) parameter. Both sensitivity parameters predict 50% efficacy near 0.1X dose whereas maximum amplitude parameters predict 50% efficacy near 1X. **C**: Comparison of ERG b-wave amplitude evoked by a 0.1 log scot-cd.s.m^{-2} flash in treated (left) eyes versus untreated (right) eyes. Dashed line represents no inter-ocular difference in this parameter. Upper limit of significant inter-ocular difference derived from untreated *rd12* and wt animals is shown with solid line. **D**: Treatment efficacy estimated using the interocular difference (IOD) of b-wave amplitude is similar to the IOD analysis of photoresponse sensitivity (log S) predicting 50% efficacy near 0.1X dose.

photoresponse sensivity could imply a difference in endogenous 9-*cis*-retinal production between the two mutant mice either due to genetic background [46] or due to differences in laboratory lighting conditions [35]. The differences in maximum amplitude of the photoresponses in the mutants could be due to differences in spontaneous activity of opsin or its constitutive phosphorylation [47-49]. Alternatively or additionally, the reduction in photoresponse maximum amplitude could be caused by a greater underlying degenerative component in *rd12* mice. More rapidly advancing degeneration in a mouse model may have particular value for testing therapies intended for translation to man, considering human degeneration in *RPE65*-LCA is severe compared to the models [20]. When we previously sought to determine efficacy in advanced disease using *Rpe65-/-* mice, we reared mice to nearly two years of age [20]. A shorter natural history for severe degeneration in *rd12* mice could facilitate and expedite studies that would be relevant to more severely affected humans with *RPE65*-LCA.

ERG data presentations in most reports of Rpe65-deficient mice illustrate small or non-detectable ERG b-waves to conventional stimuli [12-14,17,31-38]. With higher intensity stimuli, however, sizeable ERG b-waves are recordable in both models. We previously reported relatively large but insensitive photoreceptor responses using higher intensity light stimuli in *Rpe65-/-* mice [12,32]. These signals were also observed in *rd12* mice in the current study. On the other hand, detectable but insensitive ERG photoreceptor responses have not been reported in human *RPE65*-LCA to date [32,50-56]. Assuming the functional reserve in mice is due to endogenous 9-*cis*-retinal production [35,46], the apparent lack of such signals in human *RPE65*-LCA may point to differences in systemic and/or ocular retinoid metabolism between the two species [57].

A relationship between dose and treatment efficacy for AAV2-h*RPE65* vector has previously been reported only in the *RPE65* mutant dog [18]. In those experiments, two conventional ERG stimuli were used and b-waves were quantified at 8 levels of vector doses in 16 dogs. Of interest, 3 of these dogs were tested with the same human vector (at relative doses 0.1X, 0.3X and 1X) used in the present *rd12* mouse study. Results of the ERG experiments in the *rd12* mice confirm and extend the dog studies. Like the canine results, the mice showed dose-dependent improvement in ERG: 0.01X dose was ineffective whereas doses over the range of 0.1X to 1X showed an increasingly larger proportion of injected eyes with a statistically significant treatment effect.

ERG photoresponses provide a non-invasive estimate of the photoreceptor circulating current averaged across the retina [39,41,44,45]. The photoresponse sensitivity parameter assays the amplification gain of the photoreceptors and, all else being equal, it tracks changes in rhodopsin concentration [58]. Thus, increased photoresponse sensitivity (log S) following successful treatment, as observed in the current work, would have been the predictable consequence of increased rhodopsin production [12]. Improvements in photoresponse maximum amplitude observed at higher doses, on the other hand, may have more complex origins including increases in dark current due to reduction of the concentration of unliganded opsin causing spontaneous activation of phototransduction [32,34,49] and elongation of photoreceptor outer segments. Evidence to date suggests that both types of improvement in rod photoreceptor function are not only transmitted to secondary retinal neurons, as evidenced by b-waves, but also to higher visual centers [7,11,14,21,38,59].

Laboratory progress of ocular gene therapy in treating Rpe65 deficiency is now sufficient to begin developing analytical methods for products intended for human *RPE65*-LCA clinical trials [25]. We are unaware of any established potency assays for this specific purpose, so we started to fill this void by using a naturally-occurring animal model of the human disease, subretinal gene delivery, different doses of human grade vector product and an ERG assay for activity of the expressed gene. The ERG results are promising at this initial stage, but further work is needed. Variations in ERG responding to different doses of vector, for example, should be addressed. This is not a trivial issue because of the difficulties associated with subretinal injections in these small eyes, including uncertainty of degree of retinal detachment, amount of transduced RPE and the confounding effects of potential vector toxicity or retinal injury during this type of surgery. Vehicle only or sham controls would be worth performing in subsequent studies with the goal of teasing apart the contributions of retinal injury and degree of retinal detachment, for example, from degree of vector potency or vector toxicity in eyes with this retinal disease. With further advances of this bioassay, experiments should be conducted to quantify retinal detachment at surgery and determine the relation to retinal injury and amount of transduced RPE.

Biologic assays, and particularly in vivo ones, are recognized to be challenging [25]. Parallel exploration of other directions is thus warranted. For example, in vitro cell function assays involving quantitation of retinoid isomerase activity have been developed to reproduce the visual cycle and express mutant proteins. Results from these assays have the potential to help understand the pathogenicity of different *RPE65* mutations found in LCA [3,60,61]. It may be possible to adapt such cell systems to act as a surrogate potency assay for human grade vector, but there will be issues relating to the efficiency of vector transduction of cells in culture versus transduction of RPE in vivo that may complicate this approach. As another example, assays of biochemical phenotype in an in vivo experimental paradigm such as we used in the current work could also be of value. The mouse models are incapable of synthesizing requisite levels of 11-cis-retinal, the chromophore of visual pigments, and they accumulate retinyl esters, a substrate for Rpe65. Restoration of Rpe65 activity by AAV-mediated gene therapy reverses these results [4,14,31]. Although any assay of retinal tissue after gene therapy in the small mouse eye necessarily has the surgical uncertainties noted above, it may be desirable in the future to validate more than one in vivo potency assay of the Rpe65-deficient murine retinal response to therapy.

ACKNOWLEDGEMENTS

Supported by Macula Vision Research Foundation, Foundation Fighting Blindness NIH/NEI (EY11123, EY13729, EY17280, EY08571, NS36302, P30EY001583), Research to Prevent Blindness, Hope for Vision, Ruth and Milton Steinbach Foundation, and the Alcon Research Institute. The authors gratefully acknowledge the help with statistics from Dr. Gui-Shuang Ying, and with data processing and coordination from Ms. Sharon Schwartz, Ms. Anjani Naidu, Ms. Mary Nguyen, and Ms. Elaine Smilko.

REFERENCES

1. Jin M, Li S, Moghrabi WN, Sun H, Travis GH. Rpe65 is the retinoid isomerase in bovine retinal pigment epithelium. Cell 2005; 122:449-59.
2. Moiseyev G, Chen Y, Takahashi Y, Wu BX, Ma JX. RPE65 is the isomerohydrolase in the retinoid visual cycle. Proc Natl Acad Sci U S A 2005; 102:12413-8.
3. Redmond TM, Poliakov E, Yu S, Tsai JY, Lu Z, Gentleman S. Mutation of key residues of RPE65 abolishes its enzymatic role as isomerohydrolase in the visual cycle. Proc Natl Acad Sci U S A 2005; 102:13658-63.
4. Travis GH, Golczak M, Moise AR, Palczewski K. Diseases caused by defects in the visual cycle: retinoids as potential therapeutic agents. Annu Rev Pharmacol Toxicol 2007; 47:469-512.
5. Cremers FP, van den Hurk JA, den Hollander AI. Molecular genetics of Leber congenital amaurosis. Hum Mol Genet 2002; 11:1169-76.
6. Koenekoop RK. An overview of Leber congenital amaurosis: a model to understand human retinal development. Surv Ophthalmol 2004 Jul; 49:379-98.
7. Acland GM, Aguirre GD, Ray J, Zhang Q, Aleman TS, Cideciyan AV, Pearce-Kelling SE, Anand V, Zeng Y, Maguire AM, Jacobson SG, Hauswirth WW, Bennett J. Gene therapy restores vision in a canine model of childhood blindness. Nat Genet 2001; 28:92-5.
8. Narfstrom K, Katz ML, Bragadottir R, Seeliger M, Boulanger A, Redmond TM, Caro L, Lai CM, Rakoczy PE. Functional and structural recovery of the retina after gene therapy in the RPE65 null mutation dog. Invest Ophthalmol Vis Sci 2003; 44:1663-72.
9. Acland GM, Aguirre GD, Bennett J, Aleman TS, Cideciyan AV, Bennicelli J, Dejneka NS, Pearce-Kelling SE, Maguire AM, Palczewski K, Hauswirth WW, Jacobson SG. Long-term restoration of rod and cone vision by single dose rAAV-mediated gene transfer to the retina in a canine model of childhood blindness. Mol Ther 2005; 12:1072-82.
10. Le Meur G, Weber M, Pereon Y, Mendes-Madeira A, Nivard D, Deschamps JY, Moullier P, Rolling F. Postsurgical assessment and long-term safety of recombinant adeno-associated virus-mediated gene transfer into the retinas of dogs and primates. Arch Ophthalmol 2005; 123:500-6.
11. Aguirre GK, Komaromy AM, Cideciyan AV, Brainard DH, Aleman TS, Roman AJ, Avants BB, Gee JC, Korczykowski M, Hauswirth WW, Acland GM, Aguirre GD, Jacobson SG. Canine and human visual cortex intact and responsive despite early retinal blindness from RPE65 mutation. PLoS Med 2007; 4:e230.
12. Dejneka NS, Surace EM, Aleman TS, Cideciyan AV, Lyubarsky A, Savchenko A, Redmond TM, Tang W, Wei Z, Rex TS, Glover E, Maguire AM, Pugh EN Jr, Jacobson SG, Bennett J. In utero gene therapy rescues vision in a murine model of congenital blindness. Mol Ther 2004; 9:182-8.
13. Lai CM, Yu MJ, Brankov M, Barnett NL, Zhou X, Redmond TM, Narfstrom K, Rakoczy PE. Recombinant adeno-associated virus type 2-mediated gene delivery into the Rpe65-/- knockout mouse eye results in limited rescue. Genet Vaccines Ther 2004; 2:3.
14. Pang JJ, Chang B, Kumar A, Nusinowitz S, Noorwez SM, Li J, Rani A, Foster TC, Chiodo VA, Doyle T, Li H, Malhotra R, Teusner JT, McDowell JH, Min SH, Li Q, Kaushal S, Hauswirth WW. Gene therapy restores vision-dependent behavior as well as retinal structure and function in a mouse model of RPE65 Leber congenital amaurosis. Mol Ther 2006; 13:565-72.
15. Bemelmans AP, Kostic C, Crippa SV, Hauswirth WW, Lem J, Munier FL, Seeliger MW, Wenzel A, Arsenijevic Y. Lentiviral gene transfer of RPE65 rescues survival and function of cones in a mouse model of Leber congenital amaurosis. PLoS Med 2006; 3:e347.
16. Chen Y, Moiseyev G, Takahashi Y, Ma JX. RPE65 gene delivery restores isomerohydrolase activity and prevents early cone loss in Rpe65-/- mice. Invest Ophthalmol Vis Sci 2006; 47:1177-84.
17. Yanez-Munoz RJ, Balaggan KS, MacNeil A, Howe SJ, Schmidt M, Smith AJ, Buch P, MacLaren RE, Anderson PN, Barker SE, Duran Y, Bartholomae C, von Kalle C, Heckenlively JR, Kinnon C, Ali RR, Thrasher AJ. Effective gene therapy with nonintegrating lentiviral vectors. Nat Med 2006; 12:348-53.
18. Jacobson SG, Acland GM, Aguirre GD, Aleman TS, Schwartz SB, Cideciyan AV, Zeiss CJ, Komaromy AM, Kaushal S, Roman AJ, Windsor EA, Sumaroka A, Pearce-Kelling SE, Conlon TJ, Chiodo VA, Boye SL, Flotte TR, Maguire AM, Bennett J, Hauswirth WW. Safety of recombinant adeno-associated virus type 2-RPE65 vector delivered by ocular subretinal injection. Mol Ther 2006; 13:1074-84.
19. Jacobson SG, Boye SL, Aleman TS, Conlon TJ, Zeiss CJ, Roman AJ, Cideciyan AV, Schwartz SB, Komaromy AM, Doobrajh M, Cheung AY, Sumaroka A, Pearce-Kelling SE, Aguirre GD, Kaushal S, Maguire AM, Flotte TR, Hauswirth WW. Safety in nonhuman primates of ocular AAV2-RPE65, a candidate treatment for blindness in Leber congenital amaurosis. Hum Gene Ther 2006; 17:845-58.
20. Jacobson SG, Aleman TS, Cideciyan AV, Sumaroka A, Schwartz SB, Windsor EA, Traboulsi EI, Heon E, Pittler SJ, Milam AH, Maguire AM, Palczewski K, Stone EM, Bennett J. Identifying photoreceptors in blind eyes caused by RPE65 mutations: Prerequisite for human gene therapy success. Proc Natl Acad Sci U S A 2005; 102:6177-82.
21. Aleman TS, Jacobson SG, Chico JD, Scott ML, Cheung AY, Windsor EA, Furushima M, Redmond TM, Bennett J, Palczewski K, Cideciyan AV. Impairment of the transient pupillary light reflex in Rpe65(-/-) mice and humans with leber congenital amaurosis. Invest Ophthalmol Vis Sci 2004; 45:1259-71.
22. Roman AJ, Schwartz SB, Aleman TS, Cideciyan AV, Chico JD, Windsor EA, Gardner LM, Ying GS, Smilko EE, Maguire MG, Jacobson SG. Quantifying rod photoreceptor-mediated vision in retinal degenerations: dark-adapted thresholds as outcome measures. Exp Eye Res 2005; 80:259-72.
23. Roman AJ, Cideciyan AV, Aleman TS, Jacobson SG. Full-field stimulus testing (FST) to quantify visual perception in severely blind candidates for treatment trials. Physiol Meas 2007; 28:N51-6.
24. Fawaz FS, Elsheikh MA, Ogawa Y, Files JG, McCaman MT, Pungor E Jr. A potency assay for a replication incompetent adenovirus type 5 carrying a human fgf-4 gene. Anal Biochem 2005; 342:34-44.

25. Tuomela M, Stanescu I, Krohn K. Validation overview of bioanalytical methods. Gene Ther 2005; 12 Suppl 1: S131-8.
26. Birch DG. Surrogate electroretinographic markers for assessing therapeutic efficacy in the retina. Expert Rev Mol Diagn 2004; 4:693-703.
27. Brigell M, Dong CJ, Rosolen S, Tzekov R. An overview of drug development with special emphasis on the role of visual electrophysiological testing. Doc Ophthalmol 2005; 110:3-13.
28. Pinto LH, Enroth-Cugell C. Tests of the mouse visual system. Mamm Genome 2000; 11:531-6.
29. Dalke C, Loster J, Fuchs H, Gailus-Durner V, Soewarto D, Favor J, Neuhauser-Klaus A, Pretsch W, Gekeler F, Shinoda K, Zrenner E, Meitinger T, Hrabe de Angelis M, Graw J. Electroretinography as a screening method for mutations causing retinal dysfunction in mice. Invest Ophthalmol Vis Sci 2004; 45:601-9.
30. Pinto LH, Vitaterna MH, Siepka SM, Shimomura K, Lumayag S, Baker M, Fenner D, Mullins RF, Sheffield VC, Stone EM, Heffron E, Takahashi JS. Results from screening over 9000 mutation-bearing mice for defects in the electroretinogram and appearance of the fundus. Vision Res 2004; 44:3335-45.
31. Redmond TM, Yu S, Lee E, Bok D, Hamasaki D, Chen N, Goletz P, Ma JX, Crouch RK, Pfeifer K. Rpe65 is necessary for production of 11-cis-vitamin A in the retinal visual cycle. Nat Genet 1998; 20:344-51.
32. Van Hooser JP, Aleman TS, He YG, Cideciyan AV, Kuksa V, Pittler SJ, Stone EM, Jacobson SG, Palczewski K. Rapid restoration of visual pigment and function with oral retinoid in a mouse model of childhood blindness. Proc Natl Acad Sci U S A 2000; 97:8623-8.
33. Seeliger MW, Grimm C, Stahlberg F, Friedburg C, Jaissle G, Zrenner E, Guo H, Reme CE, Humphries P, Hofmann F, Biel M, Fariss RN, Redmond TM, Wenzel A. New views on RPE65 deficiency: the rod system is the source of vision in a mouse model of Leber congenital amaurosis. Nat Genet 2001; 29:70-4.
34. Woodruff ML, Wang Z, Chung HY, Redmond TM, Fain GL, Lem J. Spontaneous activity of opsin apoprotein is a cause of Leber congenital amaurosis. Nat Genet 2003; 35:158-64.
35. Fan J, Rohrer B, Moiseyev G, Ma JX, Crouch RK. Isorhodopsin rather than rhodopsin mediates rod function in RPE65 knockout mice. Proc Natl Acad Sci U S A 2003; 100:13662-7.
36. Rohrer B, Goletz P, Znoiko S, Ablonczy Z, Ma JX, Redmond TM, Crouch RK. Correlation of regenerable opsin with rod ERG signal in Rpe65-/- mice during development and aging. Invest Ophthalmol Vis Sci 2003; 44:310-5.
37. Pang JJ, Chang B, Hawes NL, Hurd RE, Davisson MT, Li J, Noorwez SM, Malhotra R, McDowell JH, Kaushal S, Hauswirth WW, Nusinowitz S, Thompson DA, Heckenlively JR. Retinal degeneration 12 (rd12): a new, spontaneously arising mouse model for human Leber congenital amaurosis (LCA). Mol Vis 2005; 11:152-62.
38. Nusinowitz S, Ridder WH 3rd, Pang JJ, Chang B, Noorwez SM, Kaushal S, Hauswirth WW, Heckenlively JR. Cortical visual function in the rd12 mouse model of Leber Congenital Amarousis (LCA) after gene replacement therapy to restore retinal function. Vision Res 2006; 46:3926-34.
39. Aleman TS, LaVail MM, Montemayor R, Ying G, Maguire MM, Laties AM, Jacobson SG, Cideciyan AV. Augmented rod bipolar cell function in partial receptor loss: an ERG study in P23H rhodopsin transgenic and aging normal rats. Vision Res 2001; 41:2779-97.
40. Jacobson SG, Yagasaki K, Feuer W, Roman AJ. Interocular asymmetry of visual function in heterozygotes of X-linked retinitis pigmentosa. Exp Eye Res 1989; 48:670-91.
41. Cideciyan AV, Jacobson SG. An alternative phototransduction model for human rod and cone ERG a-waves: normal parameters and variation with age. Vision Res 1996; 36:2609-21.
42. Pugh EN Jr, Falsini B, Lyubarsky AL. The origin of the major rod- and cone-drive components of the rodent electroretinogram and the effect of age and light-rearing history on the magnitude of these components. In. T.P. Williams and A.B. Thistle, Photostasis and related phenomena (pp. 93-128). New York: Plenum, 1998.
43. Robson JG, Maeda H, Saszik SM, Frishman LJ. In vivo studies of signaling in rod pathways of the mouse using the electroretinogram. Vision Res 2004; 44:3253-68.
44. Hood DC, Birch DG. The A-wave of the human electroretinogram and rod receptor function. Invest Ophthalmol Vis Sci 1990; 31:2070-81.
45. Pugh EN Jr, Lamb TD. Amplification and kinetics of the activation steps in phototransduction. Biochim Biophys Acta 1993; 1141:111-49.
46. Fan J, Wu BX, Sarna T, Rohrer B, Redmond TM, Crouch RK. 9-cis Retinal increased in retina of RPE65 knockout mice with decrease in coat pigmentationt. Photochem Photobiol 2006 Nov; 82:1461-7.
47. Van Hooser JP, Liang Y, Maeda T, Kuksa V, Jang GF, He YG, Rieke F, Fong HK, Detwiler PB, Palczewski K. Recovery of visual functions in a mouse model of Leber congenital amaurosis. J Biol Chem 2002; 277:19173-82.
48. Ablonczy Z, Crouch RK, Goletz PW, Redmond TM, Knapp DR, Ma JX, Rohrer B. 11-cis-retinal reduces constitutive opsin phosphorylation and improves quantum catch in retinoid-deficient mouse rod photoreceptors. J Biol Chem 2002; 277:40491-8.
49. Fan J, Woodruff ML, Cilluffo MC, Crouch RK, Fain GL. Opsin activation of transduction in the rods of dark-reared Rpe65 knockout mice. J Physiol 2005; 568:83-95.
50. Thompson DA, Gyurus P, Fleischer LL, Bingham EL, McHenry CL, Apfelstedt-Sylla E, Zrenner E, Lorenz B, Richards JE, Jacobson SG, Sieving PA, Gal A. Genetics and phenotypes of RPE65 mutations in inherited retinal degeneration. Invest Ophthalmol Vis Sci 2000; 41:4293-9.
51. Poehner WJ, Fossarello M, Rapoport AL, Aleman TS, Cideciyan AV, Jacobson SG, Wright AF, Danciger M, Farber DB. A homozygous deletion in RPE65 in a small Sardinian family with autosomal recessive retinal dystrophy. Mol Vis 2000; 6:192-8.
52. Lorenz B, Gyurus P, Preising M, Bremser D, Gu S, Andrassi M, Gerth C, Gal A. Early-onset severe rod-cone dystrophy in young children with RPE65 mutations. Invest Ophthalmol Vis Sci 2000; 41:2735-42.
53. Hamel CP, Griffoin JM, Lasquellec L, Bazalgette C, Arnaud B. Retinal dystrophies caused by mutations in RPE65: assessment of visual functions. Br J Ophthalmol 2001; 85:424-7.
54. Felius J, Thompson DA, Khan NW, Bingham EL, Jamison JA, Kemp JA, Sieving PA. Clinical course and visual function in a family with mutations in the RPE65 gene. Arch Ophthalmol 2002; 120:55-61.
55. Yzer S, van den Born LI, Schuil J, Kroes HY, van Genderen MM, Boonstra FN, van den Helm B, Brunner HG, Koenekoop RK, Cremers FP. A Tyr368His RPE65 founder mutation is associated with variable expression and progression of early onset retinal dystrophy in 10 families of a genetically isolated population. J Med Genet 2003; 40:709-13.
56. Paunescu K, Wabbels B, Preising MN, Lorenz B. Longitudinal and cross-sectional study of patients with early-onset severe retinal dystrophy associated with RPE65 mutations. Graefes

Arch Clin Exp Ophthalmol 2005; 243:417-26.
57. Lamb TD, Pugh EN Jr. Dark adaptation and the retinoid cycle of vision. Prog Retin Eye Res 2004; 23:307-80.
58. Thomas MM, Lamb TD. Light adaptation and dark adaptation of human rod photoreceptors measured from the a-wave of the electroretinogram. J Physiol 1999; 518 (Pt 2):479-96.
59. Jacobs JB, Dell'Osso LF, Hertle RW, Acland GM, Bennett J. Eye movement recordings as an effectiveness indicator of gene therapy in RPE65-deficient canines: implications for the ocular motor system. Invest Ophthalmol Vis Sci 2006; 47:2865-75.
60. Takahashi Y, Moiseyev G, Chen Y, Ma JX. The roles of three palmitoylation sites of RPE65 in its membrane association and isomerohydrolase activity. Invest Ophthalmol Vis Sci 2006; 47:5191-6.
61. Philp AR, Jin M, Li S, Roos BR, Iannaccone A, Weleber RG, Fishman GA, Jacobson SG, Travis GH, Stone EM. Disease-causing mutations in the RPE65 gene abolish retinoid isomerase activity. Invest. Ophthalmol. Vis. Sci. 2007;48: E-Abstract 2960.

The print version of this article was created on 18 Sep 2007. This reflects all typographical corrections and errata to the article through that date. Details of any changes may be found in the online version of the article.